Maximum Torque per Ampere Control Using Hill Climbing Method Without Motor Parameters Based on V/f Control

Jun-ichi Itoh, Takato Toi, Masakazu Kato
Nagaoka University of Technology
1603-1 Kamitomioka-cho
Nagaoka city Niigata, Japan
Tel., Fax: +81 / (258) – 47.9533.
E-Mail: itoh@vos.nagaokaut.ac.jp, t_toi@stn.nagaokaut.ac.jp, katom@stn.nagaokaut.ac.jp
URL: http://itohserver01.nagaokaut.ac.jp/itohlab/index.html

Keywords

«Permanent magnet motor», «Sensorless control»

Abstract

This paper proposes novel V/f control for interior permanent-magnet synchronous motors (IPMSMs) in order to achieve maximum torque per ampere (MTPA) control without motor parameters such as dq-axis inductance and flux linkage of a permanent magnet. The V/f control does not require either information of a rotor position or the motor parameters in order to construct the control system. However, the conventional MTPA control requires the motor parameters because the control determines the compensation voltage depending on the reactive power. On the other hand, with the proposed MTPA control, a hill climbing method is utilized. The proposed MTPA control calculates the compensation voltage depending on the output current in order to track the MTPA control point without the motor parameters. The validity of the proposed method is confirmed by the experimental results using a 3.7-kW IPMSM. From the experimental results, the magnitude of the phase current is decreased by 56% at the rated speed. Furthermore, the proposed MTPA control is effective regardless of the magnitude of the load torque.

I. Introduction

Recently, IPMSMs are widely applied to industry applications due to the attractive features; high power density, high efficiency and robust structure [1]-[3].There are basically two IPMSM control methods: field oriented control (FOC) and V/f control [4].

In the FOC, the identification of the pole position is necessary. Therefore, a position sensor is used to detect the pole position. However, it is impossible to use the position sensors in applications where such as a motor and a load are built-in systems. As a result, many sensorless FOC have been studied [5]-[10]. The sensorless FOC requires some motor parameters. When the motor parameters are fluctuated and different from the nominal values, it is necessary to measure the motor parameters or estimate them in the sensorless FOC [11]. In addition, in order to drive IPMSMs efficiently, MTPA control is widely applied. The MTPA control based on the FOC have been studied by using various methods such as injecting the current signal, estimating the maximum torque control frame or the motor parameters, and on-line estimation [12]-[14]. However, these methods as mentioned above require the motor parameters such as d-axis inductance, q-axis inductance and magnetic flux linkage of the permanent magnet. When the estimated motor parameters are different from the actual values, the output current does not become the minimum in the MTPA control based on the sensorless FOC because the estimated coordinate axes deviate from the actual dq-axis.

On the other hand, the V/f control does not require the identification of the pole position because the control depends on the frame which is calculated in the controller of the inverter. In addition, the motor parameters are basically not used in the V/f control. Some MTPA control based on the V/f control by controlling the current phase or the reactive power have been proposed [15][16]. However, the motor parameters are required in these MTPA control. Therefore, the MTPA control using the motor parameters spoils the advantage of the V/f control.

This paper proposes the MTPA control for the V/f control with a hill climbing method in order to achieve the MTPA control without the motor parameters. It is noted that the MTPA control using the hill climbing method is not effective in the sensorless FOC because the sensorless FOC requires the motor parameters in the control strategy. In addition, the variation of the d-axis current by the hill climbing method disturbs the position estimation system. This paper will be organized as follows; first, the principles of the V/f control is introduced. Next, the MTPA control based on the hill climbing method is explained. Finally, the experimental results are shown to confirm the validity and the effectiveness of the proposed method.

II. Maximum torque per ampere control method based on V/f control

A. V/f control

Fig. 1 shows the relationship between γδ-frame and dq-frame on rotating frame which is synchronized to rotating speed of the motor. In the permanent-magnet synchronous motor control, the d-axis and the q-axis are generally defined as the direction of the flux vector in the permanent magnet and the electromotive force vector, respectively. Therefore, the identification of the flux vector is important to apply in the FOC on dq-frame. On the other hand, the δ-axis is defined as the direction of the output voltage vector of the inverter and the γ-axis is defined as the δ-axis delayed by 90 degrees. Therefore, the δ-axis component represents effective components and γ-axis component represents reactive components. The γδ-frame is calculated in the controller of the inverter. In the V/f control, the pole position is unnecessary because the control algorithm utilizes the γδ-frame instead of the dq-frame [4].

The voltage equation of the IPMSM based on the dq-axis is given by (1).

$$\begin{bmatrix} v_d \\ v_q \end{bmatrix} = \begin{bmatrix} R + pL_d & -\omega_{re} L_q \\ \omega_{re} L_d & R + pL_q \end{bmatrix} \begin{bmatrix} i_d \\ i_q \end{bmatrix} + \begin{bmatrix} 0 \\ \omega_{re} \psi_m \end{bmatrix} \quad \text{(1)}$$

where v_d is the d-axis voltage, v_q is the q-axis voltage, ω_{re} is the electric angular frequency, p is the differential operator, R is the armature resistance value, L_d is the d-axis inductance value, L_q is the q-axis inductance value and ψ_m is the flux linkage of the permanent magnet. Then, the voltage equation of the IPMSM based on the γδ-axis is given by (2) [6].

$$\begin{bmatrix} v_\gamma \\ v_\delta \end{bmatrix} = \begin{bmatrix} R - \omega_1 L_{\gamma\delta} + pL_\gamma & -\omega_1 L_\delta + pL_{\gamma\delta} \\ \omega_1 L_\gamma + pL_{\gamma\delta} & R + \omega_1 L_{\gamma\delta} + pL_\delta \end{bmatrix} \begin{bmatrix} i_\gamma \\ i_\delta \end{bmatrix} + \omega_{re} \psi_m \begin{bmatrix} -\sin\delta \\ \cos\delta \end{bmatrix} \quad \text{(2)}$$

where v_γ is the γ-axis voltage, v_δ is the δ-axis voltage, i_γ is the γ-axis current, i_δ is the δ-axis current, ω_1 is the rotating speed of the γδ-frame and δ is the phase angle between the electromotive force and the output voltage, respectively. By definition, the output voltage vector v_δ is aligned on the δ-axis and the electromotive force $\omega_{re}\psi_m$ is aligned on the q-axis. Therefore, the phase angle δ is equal to the load angle. Here, L_γ, L_δ, $L_{\gamma\delta}$, L_0, L_1 are defined as (3) to (7).

$$L_\gamma = L_0 + L_1 \cos 2\delta \quad \text{(3)}$$

$$L_\delta = L_0 - L_1 \cos 2\delta \quad \text{(4)}$$

$$L_{\gamma\delta} = L_1 \sin 2\delta \quad \text{(5)}$$

$$L_0 = \frac{L_d + L_q}{2} \quad \text{(6)}$$

$$L_1 = \frac{L_d - L_q}{2} \quad \text{(7)}$$

The relationship between the γδ-axis current and the dq-axis current is given by (8) using the phase angle δ.

$$\begin{cases} i_d = i_\gamma \cos\delta - i_\delta \sin\delta \\ i_q = i_\gamma \sin\delta + i_\delta \cos\delta \end{cases} \tag{8}$$

The output torque of the IPMSM and the relationship between the electrical angular velocity and the output torque are expressed by (9) and (10), respectively. It is noted that the viscosity resistance is ignored.

$$T = P_f \{\psi_m i_q + (L_d - L_q) i_d i_q\} \tag{9}$$

$$p\omega_{re} = \frac{P_f (T - T_L)}{J} \tag{10}$$

where P_f is the number of pole pairs, T is the output torque, T_L is the load torque and J is the inertia moment of the motor. The phase angle δ is given by (11).

$$p\delta = \omega_1 - \omega_{re} \tag{11}$$

Fig. 2 shows the block diagram of the V/f control based on the γδ-frame. The control block contains the damping control and the conventional MTPA control.

In the V/f control, the δ-axis voltage command v_δ^* is given by the speed command ω_{rm}^* which is multiplied by the f/V conversion ratio, whereas the γ-axis voltage command v_γ^* is zero. The compensation voltage Δv_δ in order to achieve the MTPA control is subtracted from the δ-axis voltage command v_δ^*. The conventional MTPA control is discussed in the next section in detail. Then, the γδ-frame voltage command is converted to the three phase voltage command. When a motor is controlled by the simple V/f control based on the γδ-frame where there is no feedback control loop, the torque oscillation occurs due to the resonance between the synchronous reactance and the inertia moment of the motor. Therefore, the damping control is necessary in order to achieve the stable operation. Specifically, the damping control consists of HPF and the feedback gain K_1, and uses the δ-axis current as a reference to estimate the vibration component of the torque [15]. Then, the compensated speed command ω_1 is integrated in order to acquire the phase angle on γδ-frame θ_1^*. The phase angle θ_1^* is utilized in order to transform the component on the γδ-frame into the component on the three phase.

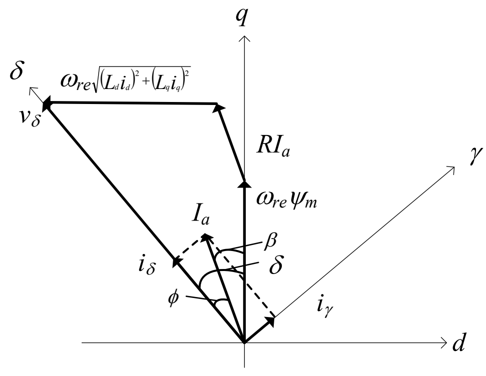

Fig. 1. Relationship between the γδ-frame and the dq-frame. The q-axis is defined as the direction of the electromotive force vector. The δ-axis is defined as the direction of the output voltage vector of the inverter.

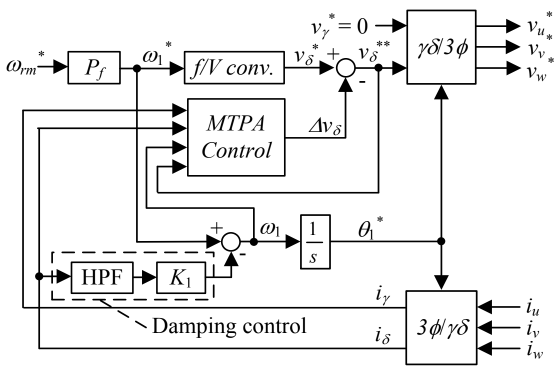

Fig. 2. V/f control based on the γδ-frame with the conventional MTPA control. The motor is controlled by the V/f control with the damping control.

B. Conventional MTPA control on V/f control

The conventional MTPA control block decides the compensation voltage Δv_δ based on the reactive power on each frame.

The reactive power on the dq-frame Q_{dq} is given by (12).

$$Q_{dq} = v_q i_d - v_d i_q \quad (12)$$

By introducing (1) into (12), the reactive power on the dq-frame Q_{dq} can be expressed as (13).

$$Q_{dq} = \omega_1 \left(L_d i_d^{\ 2} + L_q i_q^{\ 2} + \psi_m i_d \right) \quad (13)$$

Equation (13) can be rewritten as (14) by using the output current I_{a} and the current phase β.

$$Q_{dq} = \omega_1 \left(L_d I_a^{\ 2} \sin^2 \beta + L_q I_a^{\ 2} \cos^2 \beta - \psi_m I_a \sin \beta \right) \quad (14)$$

where the current phase β when the MTPA control is applied is given by (15) [17].

$$\beta = \sin^{-1}\left(\frac{-\psi_m + \sqrt{\psi_m^{\ 2} + 8\left(L_q - L_d\right)^2 I_a^{\ 2}}}{4\left(L_q - L_d\right) I_a} \right) \quad (15)$$

Let define $I_a \sin(\beta)$ as X, the reactive power in the MTPA control is given as (16).

$$Q_{dq} = \omega_1 \left\{ L_d X^2 + L_q \left(I_a^{\ 2} - X^2 \right) - \psi_m X \right\} \quad (16)$$

On the other hand, the reactive power on the γδ-axis $Q_{\gamma\delta}$ is given by (17).

$$Q_{\gamma\delta} = v_\delta i_\gamma \quad (17)$$

In case that the reactive power on the γδ-axis $Q_{\gamma\delta}$ is equal to the reactive power on the dq-frame Q_{dq} as shown in (16), the MTPA control can be achieved. Therefore, the satisfaction of (18) achieves the MTPA control during the V/f control.

$$\omega_1 \left\{ L_d X^2 + L_q \left(I_a^{\ 2} - X^2 \right) - \psi_m X \right\} = v_\delta i_\gamma \quad (18)$$

Fig. 3 shows the control block diagram of the conventional MTPA control method based on the V/f control. In order to satisfy (18), the PI controller is implemented to regulate the δ-axis voltage v_δ.

This control method does not require the information of the pole position to achieve the MTPA control. However, the control method needs the motor parameters such as the d-axis inductance L_d, the q-axis inductance L_q and the flux linkage of the permanent magnet ψ_m.

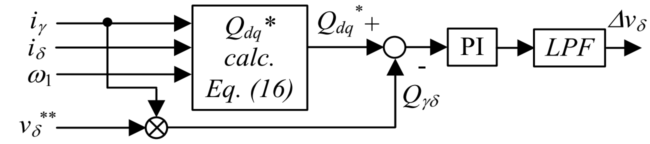

Fig. 3. Conventional MTPA control block diagram. The command value of the reactive power Q_{dq} is calculated from (16).

III. Proposed MTPA control with hill climbing method on V/f control

Fig. 4 shows the proposed control method block diagram. In the proposed method, the MTPA control is achieved by the hill climbing method which calculates the compensation voltage Δv_δ depending on the output current I_a.

By introducing (8) into (1), the relationship between the dq-axis current and the dq-axis voltage in the steady state is defined as (19).

$$\begin{bmatrix} i_d \\ i_q \end{bmatrix} = \frac{1}{R^2 + \omega_{re}{}^2 L_d L_q} \begin{bmatrix} R & \omega_{re} L_q \\ -\omega_{re} L_d & R \end{bmatrix} \begin{bmatrix} v_d \\ v_q - \omega_{re} \psi_m \end{bmatrix} \tag{19}$$

Here, because the γ-axis voltage v_γ is zero in the V/f control, the dq-axis voltage is written as (20).

$$\begin{cases} v_d = v_\delta \sin\delta \\ v_q = v_\delta \cos\delta \end{cases} \tag{20}$$

The relationship among the dq-axis current, the output current I_a and the power factor ϕ is given by (21).

$$\begin{bmatrix} i_d \\ i_q \end{bmatrix} = I_a \begin{bmatrix} \cos\delta & \sin\delta \\ -\sin\delta & \cos\delta \end{bmatrix} \begin{bmatrix} -\sin\phi \\ \cos\phi \end{bmatrix} \tag{21}$$

From (19), (20) and (21), the output current I_a is expressed as (22).

$$I_a = \sqrt{\left(Z_d{}^2 \sin^2\delta + Z_q{}^2 \cos^2\delta + 2Z^2 \sin\delta\cos\delta\right) v_\delta{}^2 - 2\omega_1 \psi_m \left(Z_q{}^2 \cos\delta + Z^2 \sin\delta\right) v_\delta + \left(\omega_1 \psi_m\right)^2 Z_q{}^2 Y^2} \tag{22}$$

where the valuables Z_d, Z_q, Z and Y are defined as (23) to (26).

$$Z_d{}^2 = R^2 + \left(\omega_1 L_d\right)^2 \tag{23}$$

$$Z_q{}^2 = R^2 + \left(\omega_1 L_q\right)^2 \tag{24}$$

$$Z^2 = R\omega_1 \left(L_q - L_d\right) \tag{25}$$

$$Y^2 = \frac{1}{R^2 + \omega_1{}^2 L_d L_q} \tag{26}$$

It is noted that the angular frequency ω_{re} is replaced as the rotating speed of the γδ-frame ω_1 because these values are same in the steady state. From (22), the output current is adjusted by the δ-axis voltage v_δ. Therefore, the MTPA control can be achieved by subtracting the compensation voltage Δv_δ from voltage command v_δ^*.

In order to confirm the validity of equations, the simulation is conducted. Table I shows the motor parameters of the IPMSM which are used in the simulation. The saliency ratio of the IPMSM is 2.5.

Fig. 5 shows the relationship between the output current I_a and the compensation voltage Δv_δ of the simulation result and the values acquired by (22). In the simulation, both results are completely corresponded. In Fig. 5, the output current I_a has the minimum value I_{a_min} at the MTPA control point.

Fig. 6 shows the flowchart of the proposed MTPA control based on the hill climbing method. Specifically, the hill climbing method is divided into four modes; Mode 1, Mode 2, Mode 3 and Mode 4. In Mode 1, the compensation voltage Δv_δ is increased to find the minimum point of the output current I_{a_min}. In Mode 2, the present value of the output current I_{a_min} is compared with the previous value of the output current I_a. When the present value of the output current I_a is higher than the threshold output current I_{a_th}, the compensation voltage Δv_δ is increased in order to maintain the minimum point of the output current. In Mode 3 and Mode 4, the compensation voltage Δv_δ is decreased and the similar operation in Mode 1 and Mode 2 are implemented. In order to alleviate the fluctuation of the output torque during the MTPA control, the fluctuation amount of the output current ΔI_a should be less than 0.1 p.u.. Therefore, the compensation voltage Δv_δ should be decided according to the fluctuation amount of the output current ΔI_a.

When the output current I_a reaches the minimum point, the hill climbing method repeats Mode 1 to Mode 4. When the variation value of the compensation voltage Δv_δ remains constant after tracking the minimum point of the output current, the current fluctuation occurs according to the torque fluctuation. Therefore, the variation value of the compensation voltage Δv_δ is decreased in Mode 4, in order that the compensation voltage Δv_δ converges to the MTPA control point. In addition, when the output current I_a exceeds the minimum value of the output current I_{a_min} by 0.2 p.u which is caused by the fluctuating load torque T_L, the parameters are initialized after waiting 1 s in order to avoid the transient state. Then, the MTPA control is resumed in order to track the MTPA control point. In this proposed MTPA control using the hill climbing method, the motor parameters are not necessary to achieve the MTPA control because the γδ-axis current is utilized.

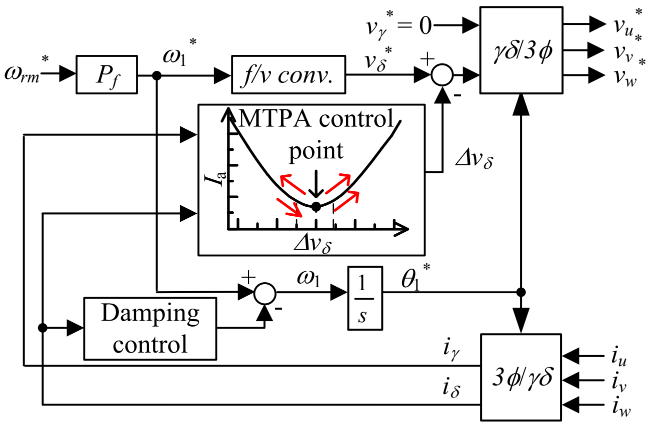

Fig. 4. V/f control based on the γδ-frame with the proposed MTPA control. The proposed method determines the compensation voltage by using the hill climbing method in order to achieve the MTPA control.

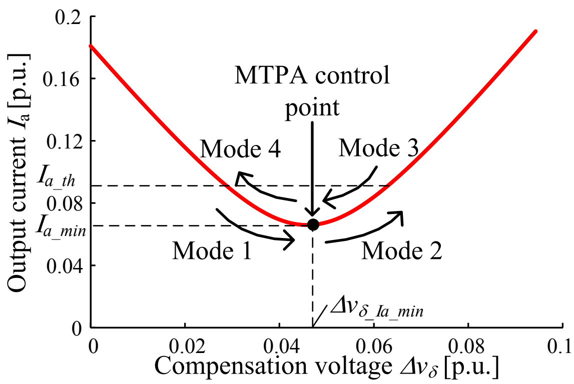

Fig. 5. Relationship between the output current I_a and the compensation voltage Δv_δ. The minimum value of the output current is achieved by controlling the compensation voltage.

Table I. Motor parameters of IPMSM.

Rated mechanical power P_m	3.7 kW	Rated torque T_{eR}	19.6 Nm
Electromotive force e_q	151 V	Winding resistance R_w	0.693 Ω
Rated voltage V_n	180 V	d, q-axis inductance L_d, L_q	6.2 mH, 15.3 mH
Rated current I_n	14 A	Inertia moment J	0.0212 kgm^2
Synchronous speed ω_s	1800 r/min	Number of pole pairs P_f	3

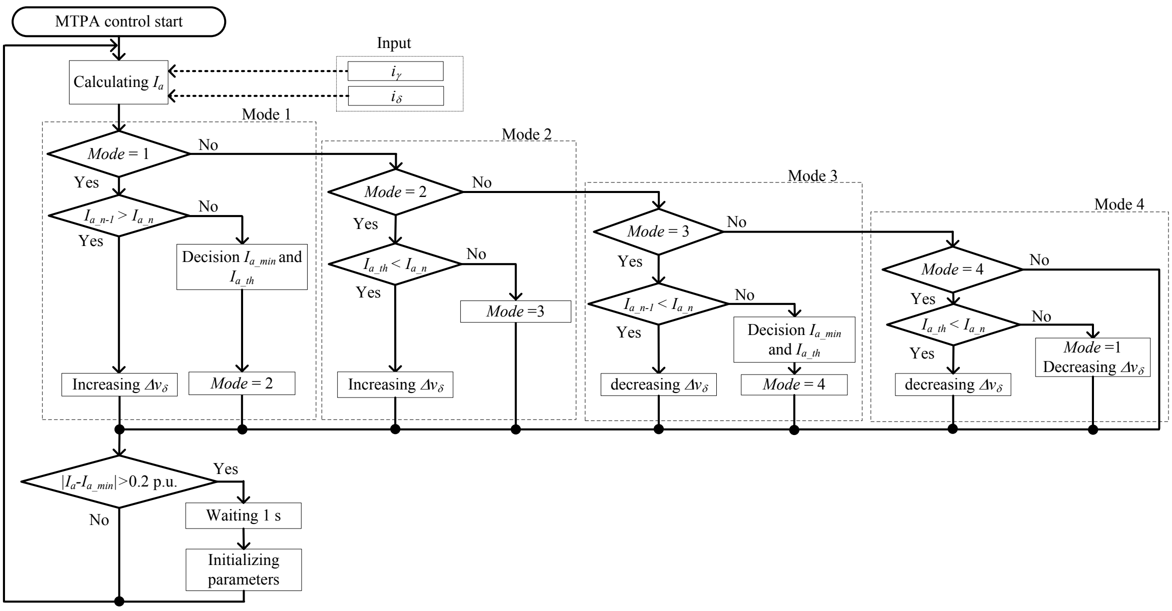

Fig. 6. Flowchart of proposed MTPA control based on the hill climbing method. This control is divided into four modes. The compensation voltage is decreased or increased depending on the relationship between the output current at previous and present calculation periods. When the output current I_a exceeds the minimum value of the output current I_{a_min} by 0.2 p.u, the parameters are initialized in order to resume the MTPA control.

IV. Experimental results

Fig. 7 shows the experimental system. The tested IPMSM is driven by a two-level inverter. In addition, a load motor is used to provide a constant torque. The information of the magnet pole position is acquired from a Hall Effect sensor to calculate the dq-axis current. It is noted that this information of the magnet pole position is not used to control the motor. The motor parameters of the experiment is shown in Table I. The parameters are same as in the simulation.

Fig. 8 shows the experimental waveforms when the proposed method is applied at 1800 r/min (1 p.u.). From Fig. 8, as mentioned above, the hill climbing method repeats Mode 1 to Mode 4 after tracking the MTPA point. Therefore, the compensation voltage Δv_δ are almost corresponded with those of the conventional method because the fluctuation amount of the compensation voltage Δv_δ is decreased in order to prevent the output torque T from fluctuating. In order to prevent the fluctuation amount of the output current from exceeding 0.1 p.u., the fluctuation amount of the compensation voltage Δv_δ is 0.02 p.u.. It should be noted that the motor parameters are used in the conventional method, whereas, the proposed MTPA control is achieved by the hill climbing method without motor parameters. Specifically, the U-phase current are reduced by 56% (from 0.18 p.u. to 0.07 p.u.) at 1.6 Nm (0.08 p.u.). Therefore, the copper loss will be reduced by 85% at most. In Fig. 8 and 9, when the load torque is increased, the compensation voltage Δv_δ is slightly decreased at each load torque T_L.

Fig. 9 shows the waveforms of the dq-axis current, the output current I_a and the U-phase current at 1800 r/min. From Fig. 11, it is understood that the d-axis current is drastically reduced, whereas, the q-axis current do not change after applying the proposed MTPA control. Specifically, the d-axis current are reduced by 91% (from 0.15 p.u. to 0.01 p.u.) at 1.6 Nm. In Fig. 11, each d-axis current becomes almost zero after applying the proposed MTPA control. Therefore, the MTPA control achieves the same results as the zero d-axis current control in the condition such as high speed and light load with the motor which the saliency ratio is 2.5.

Fig. 10 shows the amplitude of the output current I_a when the load torque T_L is varied at the rated speed of 1800 r/min and at 900 r/min (0.5 p.u.). From the both graphs, the amplitude of the output current with the proposed method is almost corresponded with the theoretical value. Therefore, the proposed method achieves the MTPA control regardless of the load torque T_L. At the light load, the q-axis current is relatively small against the d-axis current. When the load torque is increased, the proportion of the d-axis current to the q-axis current decreases because the q-axis current becomes large depending on the load torque T_L. Therefore, the MTPA control is more effective at the light load than at the heavy load.

Fig. 11 shows the waveforms of the output torque T, the rotating speed, the output current I_a and the compensation voltage Δv_δ when the load torque T_L is stepped at the steady speed with the proposed MTPA control. The rotating speed is varied 1800 r/min (1 p.u.), 1440 r/min (0.8 p.u.) and 1080 r/min (0.6 p.u.), respectively. As mentioned above, the compensation voltage Δv_δ is decided in order not to exceed the fluctuation amount ΔI_a of 0.1 p.u.. Therefore, the MTPA control is resumed when the output current ΔI_a fluctuates 0.2 p.u. including the current ripple. In addition, the MTPA control should not be activated again during the transient state which is caused by the stepped load torque T_L because the output current I_a needs to be fluctuated depending on the compensation voltage Δv_δ. From Fig. 11, the MTPA control is achieved because the transient state is avoided in case that the load torque T_L is stepped up. In addition, although the transient state is not avoided, the MTPA control is also achieved when the load torque T_L is stepped down. When the load torque T_L is stepped down, the output current decreases according to the load torque T_L. Therefore, the transient state does not need to be considered because the operating point approaches the MTPA control point automatically.

From these results, the validity of the V/f control using the hill climbing method is confirmed.

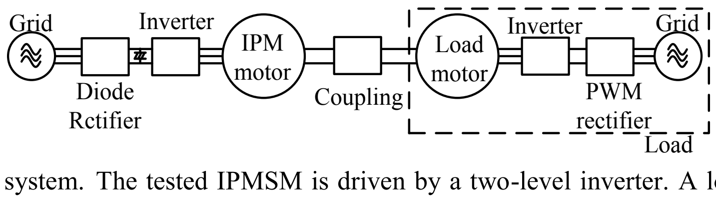

Fig. 7. Experimental system. The tested IPMSM is driven by a two-level inverter. A load motor is used to provide a constant torque.

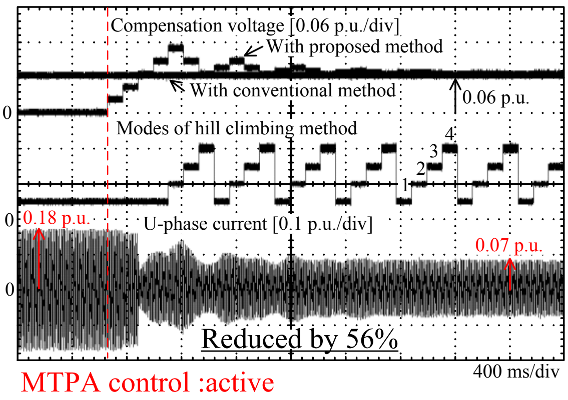

(a) At 1.6 Nm (0.08 p.u.).

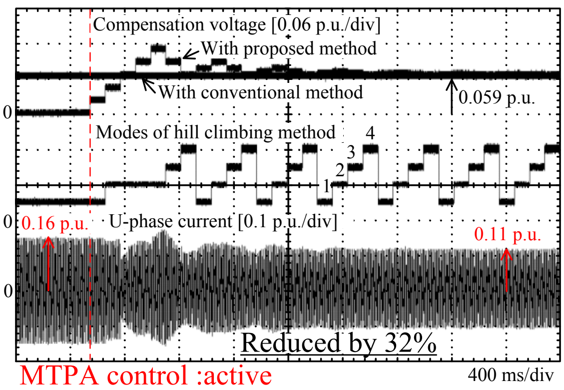

(b) At 2.4 Nm (0.12 p.u.).

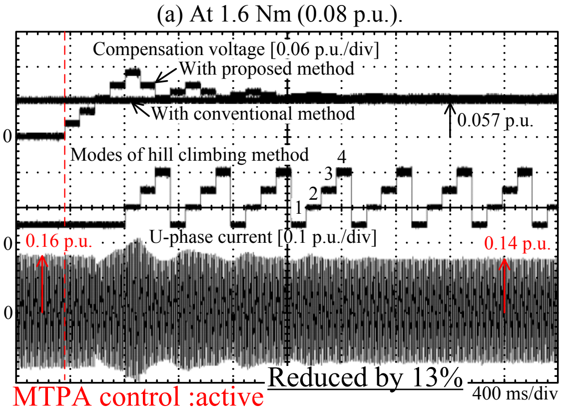

(c) At 3.4 Nm (0.17 p.u.).

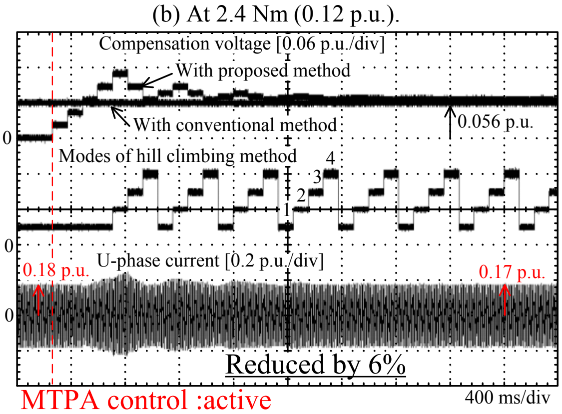

(d) At 4.0 Nm (0.20 p.u.).

Fig. 8. Waveforms of the compensation voltage of each method, modes of the hill climbing method and the U-phase current at the rated speed. The compensation voltage of each method is almost corresponded with the conventional method. The U-phase current are decreased by 56%, by 32% by 13% and by 6% at the each load torque, respectively.

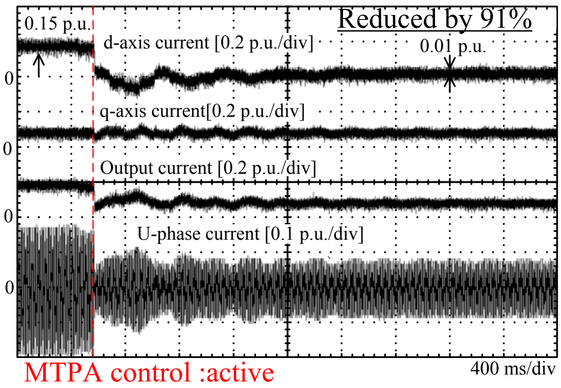

(a) At 1.6 Nm (0.08 p.u.).

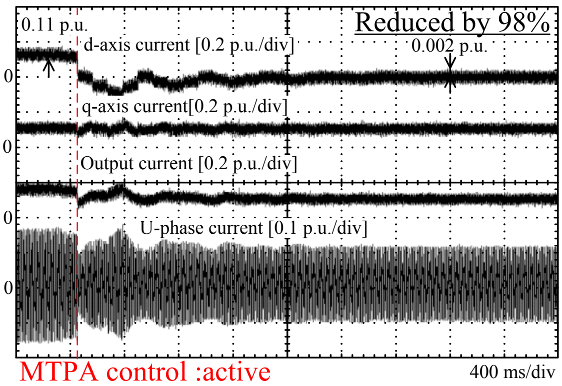

(b) At 2.4 Nm (0.12 p.u.).

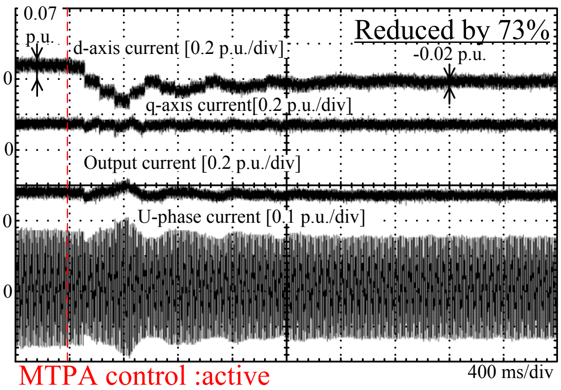

(c) At 3.5 Nm (0.18 p.u.).

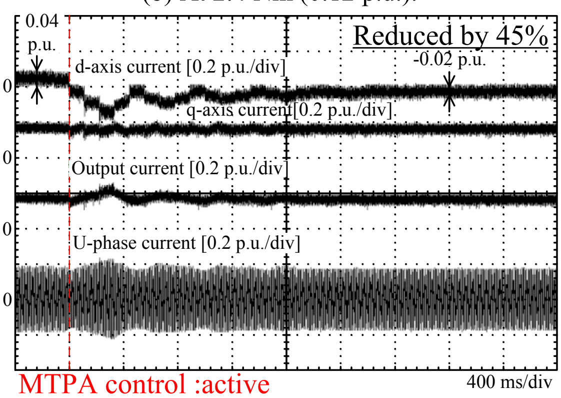

(d) At 4.0 Nm (0.20 p.u.).

Fig. 9 Waveforms of the dq-axis current, the output current and the U-phase current at the rated speed. At the steady state, the d-axis current is decreased by 91%, by 98%, by 73% and by 45% compared to the values without the MTPA control, respectively.

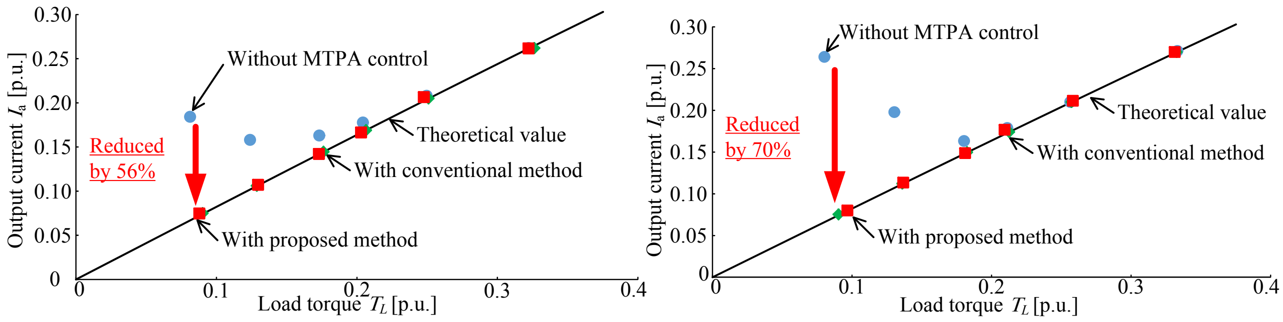

(a) At 1800 r/min (1 p.u.).

(b) At 900 r/min (0.5 p.u.).

Fig. 10. Relationship between the load torque T_L and the output current I_a with/without the MTPA control at 1800 r/min (1 p.u.) and 900 r/min (0.5 p.u.). The output current after applying the MTPA control are almost corresponded to the theoretical calculation both the proposed and the conventional method regardless of the load torque T_L.

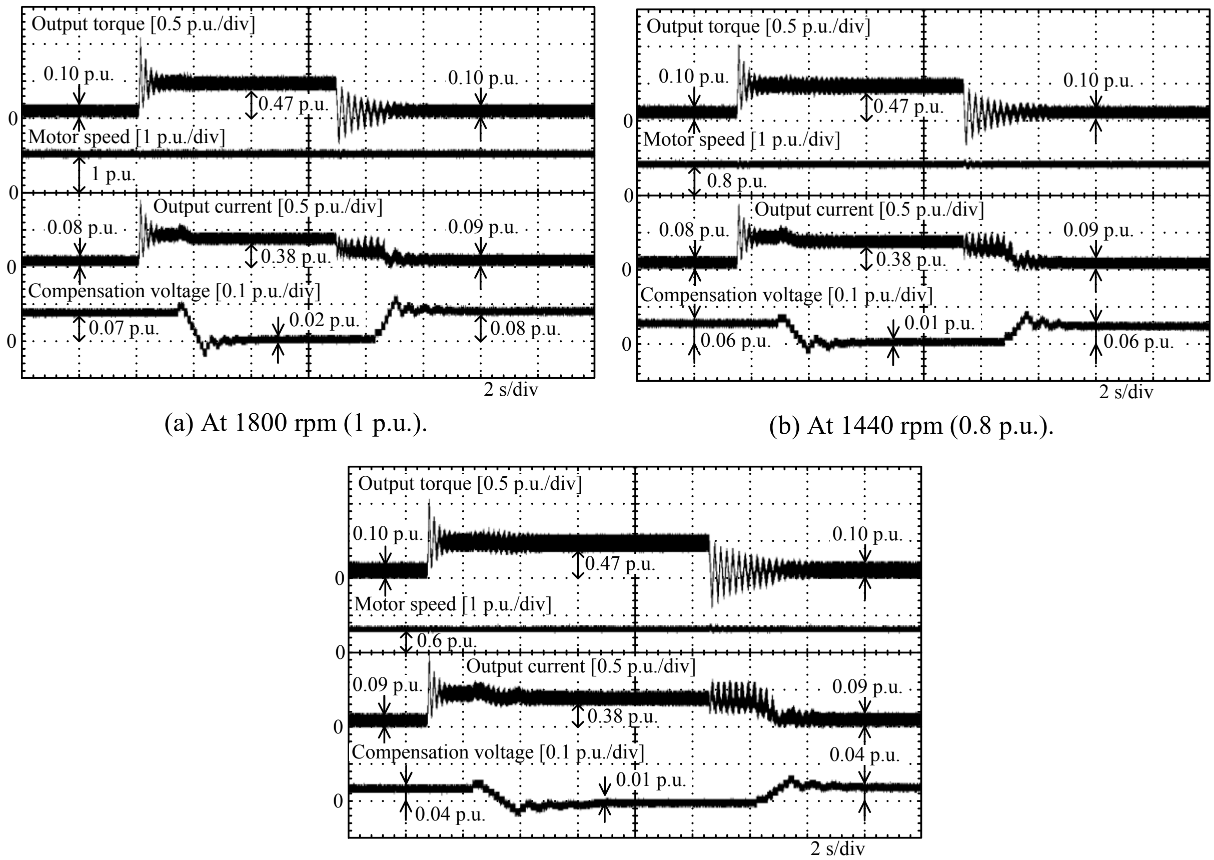

(a) At 1800 rpm (1 p.u.).

(b) At 1440 rpm (0.8 p.u.).

(c) At 1080 rpm (0.6 p.u.).

Fig. 11. Waveforms of the output torque T, the rotating speed, the output current I_a and the compensation voltage Δv_δ when the load torque T_L is stepped at the steady speed. The compensation Δv_δ voltage is varied depending on the load torque T_L in order to track the MTPA control point.

V. Conclusion

This paper discusses the V/f control which utilizes the MTPA control based on the hill climbing method. In the proposed method, the MTPA control without motor parameters is achieved. The proposed MTPA control is compared with the conventional MTPA control. From the experimental results, the phase current is decreased by 56% at the rated speed of 1800 r/min. In addition, the proposed method accomplishes the MTPA control regardless of the load torque. As a result, the validity of the proposed method is confirmed through the experimental results.

In future work, the relationship between the variation value of the compensation voltage Δv_δ and the hill climbing method will be clarified in order to accomplish the MTPA control in minimum convergence time.

References

[1] S. Kim, Y. Yoon, S. Sul, K. Ide: “Maximum Torque per Ampere (MTPA) Control of an IPM Machine Based on Signal Injection Considering Inductance Saturation”, IEEE Trans. on Power Electronics, Vol. 28, No. 1, pp. 488-497, (2013)

[2] R. Tanabe, K. Akatsu: “Advanced Torque and Current Control Techniques for PMSMs with a Real-time Simulator Installed Behavior Motor Model”, IEEJ Journal of Industry Applications, Vol. 5, No. 2, pp. 167-173, (2016)

[3] T. Zanma, M. Morimoto, K. Yubai: “Suppression of harmonic Current for IPMSM using Generalized Repeatitive Control”, IEEJ Journal of Industry Applications, Vol. 3, No. 3, pp. 214-220, (2014)

[4] J. Itoh, N. Nomura, H. Ohsawa: “A comparison between V/f control and position-sensorless vector control for the permanent magnet synchronous motor”, in Proc. Power Conversion Conf., Vol. 3, pp. 1310-1315, (2002)

[5] M. J. Corley, R. D. Lorenz: “Rotor position and velocity estimation for a salient-pole permanent magnet synchronous machine at standstill and high speeds”, IEEE Trans. on Industry Applications, Vol. 34, No. 4, pp. 784-789, (1998)

[6] Z. Chen, M. Tomita, S. Doki, S. Okuma: “An extended electromotive force model for sensorless control of interior permanent-magnet synchronous motors” IEEE Trans. on Industrial Electronics, Vol. 50, No.2, pp. 288-295, (2003)

[7] S. Morimoto, M. Sanada, Y. Takeda: “Mechanical Sensorless Drives of IPMSM With Online Parameter Identification”, IEEE Trans. on Industry Applications, Vol. 42, No.5, (2006)

[8] M. Hasegawa, S. Yoshioka, K. Matsui: “Position Sensorless Control of Interior Permanent Magnet Synchronous Motors Using Unknown Input Observer for High-Speed Drives”, IEEE Trans. on Industry Applications, Vol. 45, No. 3, pp. 938-946, (2009)

[9] K. Tobari, Y. Iwaji: “Quick-Response Technique for Simplified Position Sensorless Vector Control in Permanent Magnet Synchronous Motors”, IEEJ Journal of Industry Applications, Vol. 4, No. 5, pp. 582-588, (2015)

[10] T. Suzuki, M. Hasegawa, M. tomita, S. Doki: “Initial Position Estimation for IPMSMs Using Comb Filters and Effects on Various Injected Signal Frequencies”, IEEJ Journal of Industry Applications, Vol. 4, No. 3, pp. 204-211, (2015)

[11] X. Ji, T. Noguchi: “Online q-axis Inductance Identification of IPM Synchronous Motor Based on Relationship between Its Parameter Mismatch and Current”, IEEJ Journal of Industry Applications, Vol. 4, No. 6, pp. 730-731, (2015)

[12] S. Bolognani, R. Petrella, A. Prearo: “Automatic Tracking of MTPA Trajectory in IPM Motor Drives Based on AC Current Injection”, IEEE Trans. on Industry Applications, Vol. 47, No. 1, pp.105 -114, (2011)

[13] Y. Abdel-Rady, T. K. Lee: “Adaptive Self-Tuning MTPA Vector Controller for IPMSM Drive System”, IEEE Trans. on Energy Conversation, Vol. 21, No. 3, pp. 636-644, (2006)

[14] Y. Kang, H. Jeong. K. Lee, D. Lee, J. Kim: “Simple Estimation Scheme for Initial Rotor Position and Inductance for Effective MTPA-Operation in Wind-Power Systems using an IPMSM”, Journal of Power Electronics, Vol. 10, No. 4, pp. 396-404, (2010)

[15] J. Itoh, Y. Nakajima, G. T. Chiang: “Maximum Torque per Ampere and Maximum Efficiency Control Methods based on V/f control for IPM Synchronous Motor”, IEEEJ Journal of Industry Applications, pp. 112-120, (2014)

[16] Z. Tang, X. Li, S. Dusmez, B. Akin: “A New V/f Based Sensorless MTPA Control for IPMSM Drives”, IEEE Trans. on Power Electronics, Vol. 37, No. 2, pp. 548-558, (2015)

[17] T. M. Jahns, G. B. Kliman, T. W. Neumann: “Interior Permanent-Magnet Synchronous Motors for Adjustable-Speed Drives”, IEEE Trans. on Industry Applications, Vol. IA-22, No.4, pp. 738-747, (1986)